

**Original Article**

**The *in vivo* Assessment of Mechanical Loadings on Pectoral Pacemaker  
Implants**

Michael Hamman de Vaal<sup>1</sup>, James Neville<sup>2</sup>, Jacques Scherman<sup>1</sup>, Peter Zilla<sup>1</sup>, Micah Litow<sup>3</sup>,  
Thomas Franz<sup>1\*</sup>

<sup>1</sup>Cardiovascular Research Unit, Chris Barnard Department of Cardiothoracic Surgery,  
University of Cape Town, Cape Town, South Africa

<sup>2</sup>Cardiac Rhythm Disease Management, Medtronic Inc, Minneapolis, MN, USA

<sup>3</sup>Neuromodulation Division, Medtronic Inc, Minneapolis, MN, USA

\*Send correspondence to:

Dr Thomas Franz

Cardiovascular Research Unit

Faculty of Health Sciences

University of Cape Town

Private Bag X3, 7935 Observatory, South Africa

Tel: +27-21-406 6418; Fax: +27-21-448 5935

E-mail: thomas.franz@uct.ac.za

## Abstract

Reduced sizes of implantable cardiac pacemakers and clinical advances have led to a higher feasibility of using such devices in younger patients including children. Increased structural demands deriving from reduced device size and more active recipients require detailed knowledge of *in vivo* mechanical conditions to ensure device reliability. Objective of this study was the proof of feasibility of a system for the measurement of *in vivo* mechanical loadings on pacemaker implants. The system comprised: implantable instrumented pacemaker (IPM) with six force sensors, accelerometer and radio-frequency (RF) transceiver; RF data logging system and video capture system. Three *Chacma* baboons ( $20.6 \pm 1.15$  kg) received one pectoral sub-muscular IPM implant. After wound healing, forces were measured during physical activities. Forces during range-of-motion of the arm were assessed on the anaesthetized animals prior to device explantation. Mass, volume and dimensions of the excised *Pectoralis major* muscles were determined after device explantation. Remote IPM activation and data acquisition were reliable in the indoor cage environment with transceiver distances of up to 3m. Sampling rates of up to 1000 Hz proved sufficient to capture dynamic *in vivo* loadings. Compressive forces on the IPM in conscious animals reached a maximum of  $77.2 \pm 54.6$  N during physical activity and were  $22.2 \pm 7.3$  N at rest, compared to  $34.6 \pm 15.7$  N maximum during range-of-motion and  $13.4 \pm 3.3$  N at rest in anaesthetized animals. The study demonstrated the feasibility of the developed system for the assessment of *in vivo* mechanical loading conditions of implantable pacemakers with potential for use for other implantable therapeutic devices.

**Keywords:** Implantable device, *in vivo* force, mechanical loading, pacemaker, ICD, IPG

## Abbreviations

$A_T$	Total area of principal surface of IPM
$A_{Si}$	Surface area of force sensor cover plate
ETO	Ethylene Oxide
$F_{Si}$	Transverse force acting on force sensor i
$F_T$	Transverse force acting on IPM
$F_{T,rest}$	Transverse force on IPM at rest
ICD	Implantable cardioverter defibrillator
IPG	Implantable pulse generator
IPM	Implantable instrumented pacemaker
$L_m$	Length of <i>Pectoralis major</i> along the estimated line of action
$M_m$	Mass of <i>Pectoralis major</i>
PC	Personal computer
$R^2$	Coefficient of determination
RF	Radio frequency
ROM	Range of motion
$t_m$	Thickness of <i>Pectoralis major</i> at the location of the IPM implant
$V_m$	Volume of <i>Pectoralis major</i>
$V_{rest}$	Sensor voltage at rest
$\Delta F_T$	Difference in transverse force

## INTRODUCTION

Implantable cardiac rhythm assist devices have been used extensively for the therapy of patients with cardiac arrhythmias. These devices have been shown to reduce mortality in high-risk patient populations (Maisel et al., 2006) and to significantly increase clinical benefits for the treatment of cardiac arrhythmias compared to purely pharmacological therapy (Cleland et al., 2005). The two main groups of assist devices are implantable pulse generators (IPG), i.e. pacemakers, and implantable cardioverter defibrillators (ICD).

The implantable parts of an IPG or ICD system comprise a housing that contains the generator, battery and control circuitry, and the transvenous leads. Implantation sites include the abdominal, the retro-mammary and the pectoral regions. The abdominal region is mostly used when the physical conditions of the pectoral region are inappropriate. The retro-mammary position is preferred in female patients mainly for cosmetic considerations (Kenny, 2005). Pectoral implants have been shown to cause fewer complications compared to devices in abdominal positions (Kron et al., 2001). Hence, the pectoral region has been utilized more frequently as implant site. Here, the housing is placed in a tissue pocket either subcutaneously, resting on the *Pectoralis major*, or sub/intra-muscularly between the *Pectoralis major* and the *Pectoralis minor* and rib cage, respectively (Kistler et al., 2004).

In recent years, several factors emerged that indicate an increase in the mechanical demands placed on implanted pacemakers. Technological advances have made it possible to reduce the size, in particular the thickness, of pacemakers (Furman, 2002; Maisel et al., 2006; Shmulewitz et al., 2006). This development in combination with clinical advances has increased the feasibility of implantable pacemaker technology for the use in younger patients (Antretter et al., 2003; Friedman, 1992; Furman, 2002) who are generally more active than the adult patients traditionally receiving pacemakers. The increased mechanical demands deriving from physically more active recipients and the smaller size of the structures need to

be considered during the development stage of new devices to ensure structural integrity, mechanical longevity and device reliability. The detailed knowledge of the mechanical use conditions of implantable pacemakers becomes a pre-requisite for the design process.

While IPG and ICD leads have received extensive attention with respect to reliability (Fortescue et al., 2004; Hauser et al., 2007; Kron et al., 2001; Mattke et al., 1995) and *in vivo* mechanics (Baxter and McCulloch, 2001; Zhang et al., 2003; Zhao et al., 2003), research on the *in vivo* mechanical loadings of pacemaker housing has not been reported to date. The characterization of mechanical loading conditions of pectoral pacemaker implants may potentially be studied in cadaver tests. However, such tests can only partially represent the *in vivo* conditions. The main limiting factors of cadaver tests are: the exclusively passive movements of the upper extremities, differences in tissue properties, and the absence of conscious muscle tone, breathing loads and fibrous encapsulation of the implant as part of the biological healing process. These physiological differences may be less limiting in certain situations, e.g. for the testing of mechanical loadings on the implanted device in a simulated vehicle crash where inertia and external forces are likely to dominate. For musculoskeletal, i.e. 'internal', loading conditions associated with day-to-day activities of the recipients, these differences appear to more significantly limit the efficacy of such data.

In this study, we investigated a system for the measurement of *in vivo* loading conditions of fully implanted pacemaker housings. The study utilized a non-human primate model (*Chacma* baboon) due to the anatomical similarity of the pectoral and upper thoracic region to that of a human. Most importantly, the existence of the clavicle in the baboon qualified this animal model over other mammals, e.g. hoofed species such as sheep, which lack the clavicle and demonstrate a considerably difference in locomotion pattern of the upper extremities. The study aimed at the assessment of the feasibility of the measurement system. It was performed with a small cohort of test subjects and was not primarily designed to provide data with statistical significances.

## MATERIALS AND METHODS

### *Measurement System*

The principal components of the *in vivo* measurement system comprised: 1) Implantable instrumented pacemaker (IPM), 2) Wireless radio-frequency (RF) data logging system and 3) Synchronous video capture system. The IPM (dimensions: 64 x 61 x 11 mm, volume: 29 cm<sup>3</sup>) was equipped with six custom manufactured contact force sensors with an optimal compressive force range of 18-36 N (Tekscan, Boston, MA), a three-axis accelerometer ( $\pm 10$  g full scale per axis, Freescale Semiconductor, Tempe, AZ), an RF transceiver, a micro-controller, a real-time clock and a high-energy lithium battery. These components were embedded in a medical grade epoxy cast with a shape resembling a typical commercial pacemaker housing (Fig. 1). The force sensors were distributed across one principal surface of the device and assembled with custom-made Titanium cover plates according to the specifications of the sensor manufacturer.

The RF data control and logging system comprised a custom built transceiver RF transceiver, a PC laptop (Dell Latitude, Dell, Round Rock, TX) and control software developed using LabVIEW (National Instruments Corp, Austin, TX). The transceiver and PC laptop were connected through a serial RS232 connection. RF transmission at a maximum frequency of 1000 Hz (signal quality dependent) was utilized for the remote activation of the IPM and the acquisition of data from the force sensors and the accelerometer of the IPM. By default, the IPM was dormant to preserve battery power. In order to record and transmit data, the IPM was remotely activated for a user-defined period after which it automatically returned to dormant mode. The data transmitted from the IPM were received with the second transceiver and stored on the PC laptop for subsequent analysis.

The synchronous video monitoring system consisted of a Basler A602f 1/2" CMOS camera (Basler, Ahrensburg, Germany) with Navitar DOZ-6X8.5 zoom lens (Navitar Inc, Rochester, NY). The camera was connected to the PC laptop and operated using custom LabVIEW code. Recorded video data, interlaced with the synchronous data of the force sensors, were stored on the PC laptop.

Within 24 hours prior to implantation, the IPMs underwent standard ETO sterilization (55°C, 60% relative humidity, 12 hours).

### ***Preconditioning and Calibration of Force Sensors***

After assembly of the IPM and prior to implantation, the force sensors were preconditioned for four weeks with a mild static compression load and moisture at 37°C simulating *in vivo* conditions at rest. For preconditioning, two IPMs were placed against each other with the force sensing surfaces which were separated by a 6.4mm thick sheet of static dissipating polyurethane foam (McMaster-Carr, Elmhurst, IL). The assembly was fixed with two rubber bands such that a slight compression on the force sensing surfaces was created, rapped in wet paper tissue, placed in a sealed plastic bag and stored at 37°C.

The force sensors of each IPM were calibrated repeatedly throughout the preconditioning procedure, prior to and after sterilization, as well as after explantation in order to monitor a change of sensitivity over time. The calibration performed within 4 hours after IPM explantation served as reference for the data analysis. The calibrations were performed on an Instron 5544 universal testing machine with a 500 N load cell and Merlin software (Instron Corp, Norwood, MA). The IPM was placed in a custom-build fixture. After activating the data acquisition and transmission of the IPM, a compressive force (0 to 44.5 N, cross-head speed: 0.254 mm/min) was applied with a stainless steel pin (diameter 9.5mm, flat end) to each sensor cover plate individually. The data recorded with the IPM and the Instron 5544 were analyzed, and calibration curves were generated using a custom code in MATLAB (MathWorks Inc, Natick, MA).

## ***Implantation***

This study was approved by the research ethics committee of the University of Cape Town and animal care was in accordance with institution guidelines. Three senescent *Chacma* baboons (implant mass:  $20.6 \pm 1.15$  kg) received one IPM implant unilaterally in the upper pectoral region (alternating left and right side) under full anesthesia. The devices were placed in the sub-muscularly position with the force-sensing surface facing outwards and secured in place with two sutures. The procedures were performed using standard surgical techniques for the implantation of cardiac pacemakers. A healing period of eight weeks was allowed to ensure fibrous encapsulation of the implants before the commencement of *in vivo* measurements.

## ***Animal Housing***

Ensuring an enriched environment and companionship, the animals were housed in the primate holding facilities of: a) the University of Cape Town Animal Unit for a three day acclimatization period prior to the surgical procedures and during post-implant healing, and b) the Animal Centre of the South African Medical Research Council for the remainder of the study.

## ***Measurements of in vivo Loadings***

Using the measurement system, *in vivo* loadings on the implanted IPM devices associated with activities of the animals were recorded in daily sessions of 5 to 15 minutes duration for up to six days. The measurements were performed during periods of elevated levels of physical activity of the animals prior to the routine feeding. The activities of the animals included vertical movement in the cages, pulling and pushing at cage walls and ceiling using the upper extremities, and single-arm striking. Physical activities of the animals associated with the loading events were recorded with synchronized video. The *in vivo* loading data of the physiological range of motion (ROM) of the upper extremities were acquired on

anesthetized animals. The arm/shoulder complex of the pectoral side with IPM implant was rotated predominantly in the axial, coronal and sagittal plane, respectively, to simulate isolated adduction/abduction, circumduction and elevation. Subsequently, the animals were euthanized under full anesthesia and the IPM implants were retrieved.

### ***Morphometric Measurements and Histology***

Post-mortem, the length,  $L_m$ , of the *Pectoralis major* along the estimated line of action and the thickness,  $t_m$ , of the *Pectoralis major* at the location of the IPM were recorded *in situ* using a ruler and caliper, respectively. Following excision, the mass,  $M_m$ , and volume,  $V_m$ , of the excised *Pectoralis major* were measured with a scale and by fluid displacement method, respectively. The fibrotic capsule formed around the implant and adjacent muscles tissue underwent paraffin histology and staining for Hematoxylin & Eosin and fluorescent CD68 to assess fibrotic tissue formation and inflammatory response.

### ***Data Analysis***

Data of the IPM force sensors were processed using customized software routines in MATLAB (MathWorks Inc, Natick, MA). The raw voltage data were subjected to a median filter ( $n = 7$ ) to reduce noise levels. In absence of a true and common *in vivo* reference value, the voltage at rest,  $V_{rest}$ , of the conscious animals was used as reference for the voltage-force conversion algorithm. The sensor calibration curves obtained within four hours after device explantation were identified to most closely approximate the sensor sensitivity during the *in vivo* experiments and were used for the data conversion. Assuming an equal distribution over the principal IPM surface, the transverse force  $F_T$  acting on the IPM was determined from the sum of the individual forces of the six sensors,  $F_{Si}$ , and the ratio of the total area of the IPM principal surface  $A_T$  to the sum of the areas of the sensor cover plates,  $A_{Si}$ :

$$F_T = \frac{A_T}{\sum_{i=1}^6 A_{Si}} \sum_{i=1}^6 F_{Si} \quad (1)$$

A custom peak detection algorithm in MATLAB was employed to obtain single maximum force values associated with distinct movement events. The algorithm was based on the comparison of the force value of two adjacent data points. A threshold value of  $\Delta F_T = 0.25$  N was found to be suitable to prevent loss of significant features of the force data.

### ***Statistical Analysis***

Continuous data were expressed as mean and standard deviation. Categorical data were expressed as median. Correlations were ascertained using single linear regression analysis. Statistical significance was assumed for p values smaller than 0.05.

## **RESULTS**

### ***Operation of Measurement System***

Remote activation and data acquisition were found to be reliable and repeatable for all implanted IPMs for distances of up to 3 m between the animal in the metal cage and the transceiver outside the cage. Utilizing real-time feedback from the RF data acquisition system, the signal quality was optimized by adjusting the distance and position of the transceiver relative to the cage. The operation of the force measurement and the video monitoring through integrated control software from the PC laptop ensured exact synchronization of force and video data.

### ***In vivo Loading Conditions during Voluntary Activities***

For implants 447 and 449, 20 and 19 experiments (data acquisition sessions) were conducted with a total duration of 77 and 78 minutes while implant 575 underwent 10 experiments with a total duration of 38 minutes. Histograms of the compressive force  $F_T$  measured during all experiments are presented in Fig. 2 for each implant. The maximum and median force on the IPM,  $F_T$ , during voluntary activities of the animals was on average  $77.2 \pm 54.6$  N and  $22.1 \pm$

7.0 N, respectively. The individual values of maximum and median  $F_T$  are illustrated in Fig. 3. With the animals at rest, the force on the IPM,  $F_{T,rest}$ , was 14.3, 23.7 and 28.7 N for the implants 447, 449 and 575, respectively, (single measurements without standard deviation; average  $22.2 \pm 7.3$  N).  $F_{T,rest}$  was found to be very close to the median of the force  $F_T$  during activities (presented in Fig. 3). For the 30 highest values of  $F_T$  of each IPM implant, the associated movements of the upper extremities were identified in the synchronous video data. The typical movements were pushing (against cage wall, weight bearing, landing from vertical movement), pulling (at cage walls and foraging objects), stretching (adduction, abduction and raising of arms without resistance) and striking (fast movement of arm without resistance) while some force events remained unidentified.

### ***In vivo Loadings during Range of Motion and Morphometric Measurements***

In the anaesthetized animals, the force on the IPM at rest was  $F_{T,rest} = 13.4 \pm 3.3$  N (9.8, 16.3 and 14.1 N for implants 447, 449 and 575) with the arm ipsilateral to the implant in the anatomical position. The maximum force recorded during the range of motion movements was  $34.6 \pm 15.7$  N. For most of the positions of the arm, the forces on the IPM were only marginally larger than the force at rest, indicated by values of the ratio  $F_T/F_{T,rest}$  close to unity (see Fig. 4). For two implants, a marked increase of the force on the IPM of 4.0 and 2.9 times  $F_{T,rest}$  was recorded in the adducted position of the arm. The morphometric measurements of the *Pectoralis major* muscles are summarized in Table 2.

## DISCUSSION

The feasibility of the wireless *in vivo* measurement system in terms of data acquisition capabilities, force measurement capabilities and versatility of the instrumented pacemakers was successfully demonstrated in this study. The radio-frequency activation of implanted IPMs and transmission of *in vivo* force and acceleration data were reliable and repeatable in the indoor cage environment with transceiver distances up to 3m. The measurement system facilitated signal-quality dependent sampling rates of up to 1000 Hz that were sufficiently high to capture the dynamic *in vivo* loading conditions. The signal quality was generally very good and most remnant noise was sufficiently removed with a median filter and a custom high-pass filter. The piezo-resistive force sensing technology proved to be dynamically responsive and to provide a repeatable and accurate force measurement under experimental *in vivo* conditions. Responsiveness of the sensors under *in vivo* loading conditions was found to be very good. The experimental conditions of this study were conducive for good repeatability and accuracy of the force measurements with the employed sensor technology (Brimacombe et al., 2009). This included sufficient conditioning of sensors to experimental conditions, repeated post-explantation calibration providing multiple points on the calibration curve and a repeatable reference measurement.

The force events recorded with the different IPMs were of similar Gauss-type amplitude distribution with a gradual tail towards larger magnitudes (Fig. 2). The majority of  $F_T$  events were close to  $F_{T,rest}$  whereas events with maximum  $F_T$  amplitude occurred very infrequently. For all three implants, 95% of the  $F_T$  data was found to lie approximately between  $0.8 F_{T,rest}$  (2.5<sup>th</sup> percentile) and  $1.2 F_{T,rest}$  (97.5<sup>th</sup> percentile). The maximum amplitude of  $F_T$  was found to be between two- and five-fold  $F_{T,rest}$  for the different IPM implants. The comparison of  $F_{T,max}$  of the different implants was somewhat restricted due to the fact that maximum voluntary contraction, generally used in experiments with human volunteers, could not be

confirmed in these experiments on animals. However, a strong correlation of  $F_{T,rest}$  with the volume  $V_m$  of the *Pectoralis major* ( $R^2 = 0.99$ ,  $p = 0.008$ ) in combination with the uncontrolled movements of the animals justified the variation of  $F_{T,max}$  between the three IPMs.

Although the intensity of movements determined the magnitude of the loading on the device, a clear ranking with respect to force amplitude could neither be ascertained for type of movement (e.g. pushing, pulling, etc) for the conscious animals (Table 1) nor for the position of the arm for the ROM experiments on the anaesthetized animals (excluding the adducted position, Fig. 4).

The force on the implanted IPM was caused by a combination of compression by, and tension in, the surrounding anatomical structures. More specifically, the force was caused by a combination of the extreme positions of the arm movement, generating tension in the fibrous encapsulation of the implanted IPM and the strength of *Pectoralis major* contraction. This finding was supported by the results of the ROM experiments, which yielded peak forces caused by stretching and compressing of the *Pectoralis major*, respectively (Fig. 4). However, not all extreme positions of the arm caused peak forces. Circumduction, for example, resulted in a fluctuating rather than continuous  $F_T$  response which was ascribed to the fusion of the fibrotic encapsulation and the surrounding anatomical structures. The force on the IPM was affected by the position of the upper arm.

The contribution of the muscle tone to the force on the IPM implants was evident from a decrease in resting force  $F_{T,rest}$  of between 31% and 51% in the anaesthetized animals compared to the conscious animals. This outcome indicated the effect of muscle tone on *in vivo* forces on implants which typically cannot be captured in cadaver experiments.

Although the baboon model exhibits close anatomical similarity to humans with respect to the shoulder/arm complex which enables similar locomotion of the arm, the overall locomotion patterns of the animals observed in this study were somewhat different from

those associated with typically activities of humans. This may potentially be addressed in future research by training and motivating the animals to perform movements and activities that more closely resemble those of humans. This was not attempted during the presented study due to the focus on system feasibility. In addition, maximum voluntary contraction, a parameter often employed in musculoskeletal research involving volunteers and patients, was not utilized in this study as this activity is difficult, if not impossible, to achieve with animals. Here, alternative approaches and techniques will be required to facilitate the translation from animal subjects to humans. These may include electrical stimulation of the pectoral muscle which can be achieved minimally invasive both in animals and volunteers.

## CONCLUSIONS

While the feasibility of the measurement system was demonstrated for pectoral sub-muscular pacemaker implants, the system can be beneficial for the study of the *in vivo* mechanical loading conditions in other anatomical positions, e.g. pectoral sub-cutaneous implants, and for other implantable or wearable medical devices. Beyond the focus on internal forces of the musculoskeletal system on implants, the system will also be useful for the assessment of handling forces, e.g. during implantation, and mechanical loads originating from external sources. Although the experimental design of the study was tailored towards proof of feasibility and not to provide statistically sound power, the experimental findings can provide essential supplementation to cadaver studies. These findings specifically include the influences on mechanical *in vivo* loadings not present in cadavers such as the muscle tone and loads due to fibrotic encapsulation of the implants. Follow up research planned includes a study with a larger number of animal subjects utilizing an experimental design similar to that presented in this paper, as well as a study on the correlation between the compressive force on the pectoral implant and the in-line force of the *Pectoralis major*.

## CONFLICT OF INTEREST STATEMENT

MHdV, JS, PZ and TF do not have conflicts of interest. JN and ML are inventors on a patent application “Implantable Medical Device Including Mechanical Stress Sensors”, P0023322.00.

## REFERENCES

- Antretter, H., Colvin, J., Schweigmann, U., Hangler, H., Hofer, D., Dunst, K., Margreiter, J., Laufer, G., 2003. Special problems of pacing in children. *Indian Pacing and Electrophysiology Journal* 3, 23-33.
- Baxter, W.W., McCulloch, A.D., 2001. In vivo finite element model-based image analysis of pacemaker lead mechanics. *Medical Image Analysis* 5, 255-270.
- Brimacombe, J.M., Wilson, D.R., Hodgson, A.J., Ho, K.C.T., Anglin, C., 2009. Effect of calibration method on tekscan sensor accuracy. *Journal of Biomechanical Engineering* 131, 034503-034504.
- Cleland, J.G.F., Daubert, J.-C., Erdmann, E., Freemantle, N., Gras, D., Kappenberger, L., Tavazzi, L., 2005. The effect of cardiac resynchronization on morbidity and mortality in heart failure. *New England Journal of Medicine* 352, 1539-1549.
- Fortescue, E.B., Berul, C.I., Cecchin, F., Walsh, E.P., Triedman, J.K., Alexander, M.E., 2004. Patient, procedural, and hardware factors associated with pacemaker lead failures in pediatrics and congenital heart disease. *Heart Rhythm* 1, 150-159.
- Friedman, R.A., 1992. Pacemakers in children: Medical and surgical aspects. *Texas Heart Institute Journal* 19, 178-184.
- Furman, S., 2002. The future of the pacemaker. *Pacing and Clinical Electrophysiology* 25, 1-2.

- Hauser, R.G., Hayes, D.L., Kallinen, L.M., Cannon, D.S., Epstein, A.E., Almquist, A.K., Song, S.L., Tyers, G.F.O., Vlay, S.C., Irwin, M., 2007. Clinical experience with pacemaker pulse generators and transvenous leads: An 8-year prospective multicenter study. *Heart Rhythm* 4, 154-160.
- Kenny, T., 2005. *The nuts and bolts of cardiac pacing*. Blackwell Futura, Malden.
- Kistler, P.M., Eizenberg, N., Fynn, S.P., Mond, H.G., 2004. The subpectoral pacemaker implant: It isn't what it seems. *Pacing and Clinical Electrophysiology* 27, 361-364.
- Kron, J., Herre, J., Renfro, E.G., Rizo-Patron, C., Raitt, M., Halperin, B., Gold, M., Goldner, B., Wathen, M., Wilkoff, B., Olarte, A., Yao, Q., 2001. Lead- and device-related complications in the antiarrhythmics versus implantable defibrillators trial. *American Heart Journal* 141, 92-98.
- Maisel, W.H., Moynahan, M., Zuckerman, B.D., Gross, T.P., Tovar, O.H., Tillman, D.-B., Schultz, D.B., 2006. Pacemaker and icd generator malfunctions: Analysis of food and drug administration annual reports. *Journal of the American Medical Association* 295, 1901-1906.
- Mattke, S., Muller, D., Markewitz, A., Kaulbach, H., Schmockel, M., Drwarth, U., Hoffmann, E., Steinbeck, G., 1995. Failures of epicardial and transvenous leads for implantable cardioverter defibrillators. *American Heart Journal* 130, 1040-1044.
- Shmulewitz, A., Langer, R., Patton, J., 2006. Convergence in biomedical technology. *Nature Biotechnology* 24, 277-280.
- Zhang, J.Y., Chen, S.J., Cooke, D.J., Hansgen, A.R., Wu, H.A., Carroll, J.D., Giudici, M., Analysis of intracardiac lead bending stresses and motion characteristics of rva versus rvs pacing leads using an innovative 3-d reconstruction technique, Summer Bioengineering Conference, Sonesta Beach Resort in Key Biscayne, Florida 2003.
- Zhao, Y., Baxter, W., Johnson, B., Schendel, M., McCarty, J., McMahon, C., Lahm, R., Sun, H., Morissette, J., Laske, T., Miller, J., The use of nonlinear fea modelling to

determine the in vivo cardiac pacing lead coils for fatigue evaluation, Summer Bioengineering Conference, Sonesta Beach Resort in Key Biscayne, Florida 2003.

## Tables

Table 1. Normalized force  $F_T/F_{T,rest}$  on IPM implants associated with movements inducing high levels of loads

<b>Movement</b>	<b><math>F_T/F_{T,rest}</math></b>			
	<b>447</b>	<b>449</b>	<b>575</b>	<b>Mean</b>
Pushing	$1.9 \pm 0.2$	$4.0 \pm 0.0$	1.8	$2.1 \pm 0.7$
Pulling	$1.7 \pm 0.0$	$4.2 \pm 0.9$	$1.7 \pm 0.3$	$2.5 \pm 1.7$
Stretching	$1.9 \pm 0.3$	-	-	-
Striking	$1.7 \pm 0.0$	-	-	-
Unidentified	$1.8 \pm 0.2$	$3.8 \pm 0.3$	$1.6 \pm 0.0$	$2.3 \pm 1.1$

Table 2. Animal masses and morphometric parameters of the *Pectoralis major* muscle

	Implant No			Mean
	447	449	575	
Animal mass [kg]	24.7	23.0	20.7	22.8 ± 2.0
<i>Pectoralis major</i>				
M <sub>m</sub> [g]	82	125	149	118.7 ± 34.0
V <sub>m</sub> [cm <sup>3</sup> ]	70	120	135	108.3 ± 34.0
t <sub>m</sub> [cm]	0.50	0.40	0.45	0.45 ± 0.05
L <sub>m</sub> [cm]	15.0	17.0	19.5	17.2 ± 2.3

## Figures

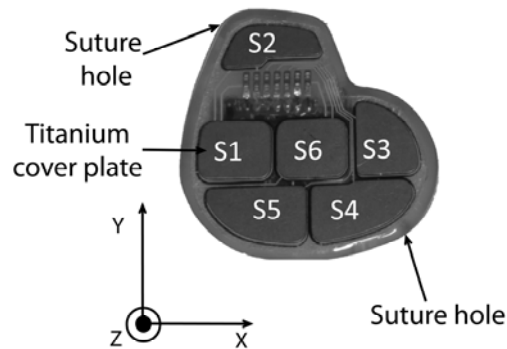


Figure 1. Photograph of instrumented pacemaker showing the Titanium cover plates of six contact forces sensors (S1 to S6). The epoxy cast featured two suture holes for fixation of the device to surrounding tissue in order to prevent migration of the implant.

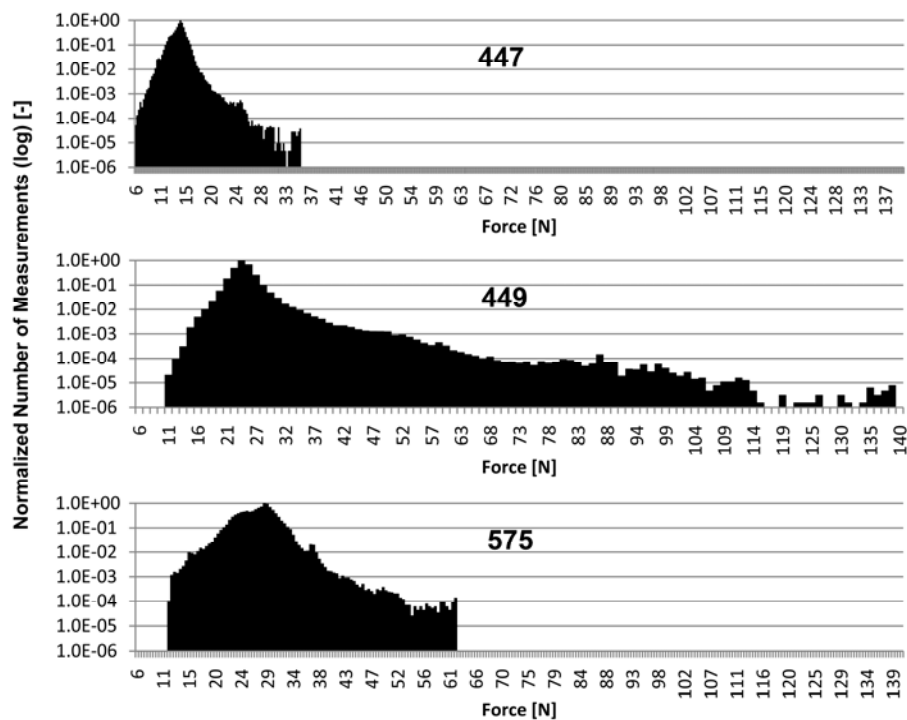


Figure 2. Histograms of force  $F_T$  measurements for the IPM implants during voluntary activities of the animals. The number of measurements was normalized to the highest number of events of a single force for each IPM device in order to account for the different total number of measurement associated with the different durations of the experiments for the three individual implants.

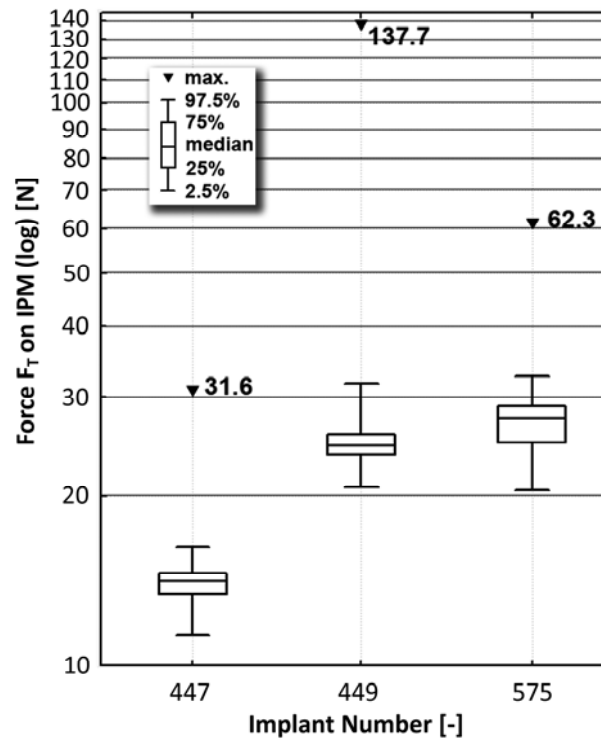


Figure 3. Box and whisker plot of the transverse force,  $F_T$ , exerted on implanted IPM devices during voluntary activities of the animals. For each IPM implant, the following  $F_T$  values are presented: Median, 25<sup>th</sup> and 75<sup>th</sup> percentile (open box), 2.5<sup>th</sup> percentile (lower whisker), 97.5<sup>th</sup> percentile (upper whisker), and maximum (triangles), see legend in insert.

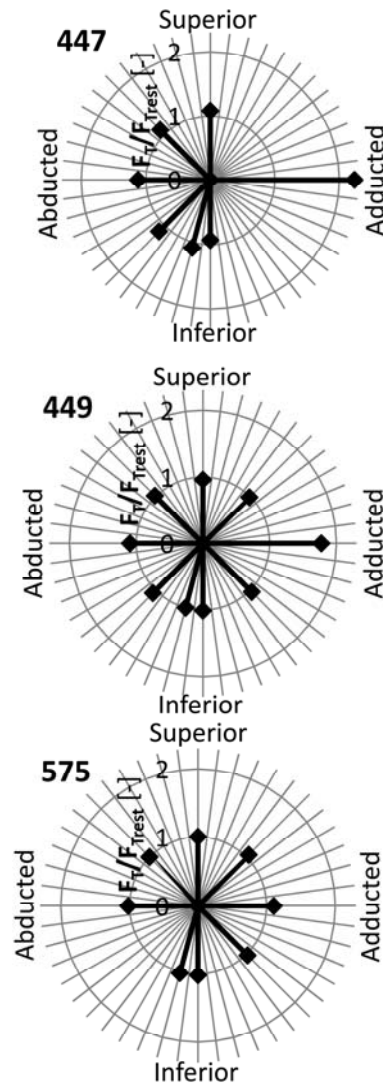


Figure 4. Polar graphs of the normalized force ,  $F_T/F_{T,rest}$ , versus position of the arm during the range of motion experiments on the anesthetized animals with IPM implants 447, 449, and 575. The centre of each graph represents the centre of rotation (shoulder). The superior, inferior, adducted and abducted anatomical positions of the arm during the range of motion are indicated in each graph.